

Closed-Loop Amplitude Modulation Control of Reacting Premixed Turbulent Jet

E. Gutmark,* T. P. Parr,† D. M. Hanson-Parr,‡ and K. C. Schadow‡
Naval Weapons Center, China Lake, California 93555

A closed-loop control system was constructed to control the initiation of reaction in a turbulent fuel/air jet at the lean flammability limit. Control authority was obtained by forcing the initial shear layer of the fuel/air mixture, thus generating small-scale vortices which improved the flame stability. The optimal forcing frequency was determined in open-loop control tests, which defined the effective range and related it to the Kelvin-Helmholtz instability of the shear layer. An amplitude modulation (AM) controller was developed using the open-loop frequency as a carrier signal. Bode and Nyquist analyses showed that the reaction is stable only in a limited range due to time lag related to the convection time of the vortices. In spite of the high noise level of this turbulent combustion system, it was possible to use linear control theory to analyze the time-averaged transfer functions. The application of lead and lag compensations was studied to extend the stability margins. The control system response to changes in operating conditions such as set-point and flow rates were compared to the open-loop control operation and found to be superior.

Introduction

COMBUSTION features are strongly coupled to the shear flow dynamics in reacting jets.¹ It was shown that shear-layer instabilities^{2,3} and coherent structures, which are evolving as a result of these instabilities, affect the reaction intensity and stability.⁴ The combination of large- and small-scale mixing in a shear layer and its location relative to the flameholder determine the location of combustion and the energy release distribution.

In certain combustor designs with adverse operational conditions (for example, low chamber pressure), combustion is initiated at a certain stand-off distance from the dump or flameholder. The delay of the onset of combustion is due to the presence of large-scale vortical structures in the shear flow and may result in high-amplitude pressure oscillations, low combustion efficiency, and narrow flammability margins.

Passive and active control methods, aimed to modify the flow pattern, were applied to premixed and diffusion flames with favorable results that stabilized the combustion and changed the regions of the chemical reaction. Gutmark et al.⁵ showed the effect of shear-layer excitation on the suppression of vortices and increased heat release in a diffusion flame. They also demonstrated an extension of the blowout limit of a premixed flame using the same technique.⁶ Similar results were obtained in a 2-D dump combustor with lean premixed flames.⁷ The periodic perturbation of the shear layer resulted in enhanced combustor performance, including higher energy release, decreased fluctuations, and improved lean blowout limit and reduced NO_x emission. These changes obtained by open-loop control suggested the possibility to use closed-loop feedback systems for flame control.

Active control methods were applied successfully in various engineering applications such as noise suppression⁸ and stabilization of compressor surge.⁹

Lang et al.¹⁰ applied the principle of "antisound"⁸ to suppress combustion instabilities in a laboratory combustor (1 kW). A microphone, located upstream of the flame, provided

the excitation signal. The signal was filtered, amplified, and phase shifted before activating a loudspeaker. The oscillations amplitude was reduced by 66 dB. The same method was applied to suppress instabilities of a 250 kW turbulent combustor.¹¹ The sound pressure level was reduced by 20 dB and a stable combustion was obtained. A similar approach with a different actuator was used by Bloxsidge et al.¹² to control reheat buzz instability in a 250 kW combustor. The instability signal was picked up by a pressure transducer, and after filtration and phase shifting was fed into a vibrator which altered the blockage to the flow, thus producing a fluctuating mass flow into the chamber. The peak pressure oscillations were reduced by 20 dB and the acoustic energy to 10% of its uncontrolled level. The same rig was used to demonstrate the effectiveness of another actuator.¹³ The oscillations were suppressed by an unsteady addition of extra fuel. A phased addition of 3% fuel reduced the peak of pressure oscillations by 12 dB. The controller enabled the rig to run at high fuel-to-air ratio, thus leading to an increase in the maximum thrust.

Gulati and Mani¹⁴ used a similar gain/phase shift controller to suppress combustion instabilities in a small-scale premixed combustor by 15 dB. They pointed out the limited gain and phase margins of the controller in the presence of multiple unstable modes in the combustor.

Closed-loop feedback systems are easier to implement in linear or quasilinear systems than in nonlinear systems. The operational conditions for the present experiments were chosen so that this requirement would be partially fulfilled. The driving force was chosen to be acoustical and the jet flow to be at a low Reynolds number. Even for such a relatively simplified system, the various physical mechanisms (acoustics, fluid dynamics, and combustion) are interacting, and the system identification process necessary for implementing feedback control is complicated.

Identification of the acoustical and fluid dynamic subsystems was done by analyzing the transfer function, which was obtained by driving the system with both white noise and a frequency-swept sine wave. The acoustical subsystem was dominated by the resonant acoustic modes of the settling chamber. These modes were subsequently filtered and amplified by the flow shear layer, whose instability characteristics are dominated by the preferred mode frequency.¹⁵

A closed-loop active combustion control system requires some feedback signal between the combustion output and the actuators which control the primary and/or secondary flows.

Received Sept. 5, 1990; revision received June 3, 1991; accepted for publication June 4, 1991. This paper is declared a work of the U.S. Government and is not subject to copyright protection in the United States.

*Research Scientist, Research Department. Member AIAA.

†Research Chemist, Research Department.

‡Supvy. Gen. Engineer, Research Department.

An indicator of combustion intensity is therefore required that is simple to implement and has a high enough frequency response to not limit the control loop. Natural flame chemiluminescence emission from radicals, specifically CH and C_2 , can be used as indicators of combustion zone location and intensity and can be monitored with simple high-time-response detectors.⁷ Flame-excited CH and C_2 apparently follow ground state CH and C_2 spatially, and chemiluminescent radiation from them is therefore a good indicator of flame front location.

The present paper describes a closed-loop control system used to stabilize the combustion at the lean flammability limit. CH and C_2 chemiluminescence is used as a flame height detector, which is used in an amplitude modulation loop to control the flow. The operation of the closed-loop system and its response to varying operational conditions are described.

Experimental Arrangement

A propane/air premixed circular reacting jet was studied (Fig. 1). The air was supplied through a 290-mm-long circular pipe with a 19-mm-diameter circular orifice exit. The propane was injected at the entrance to the pipe through multiple circumferential holes, normal to the pipe walls at a rate of 1.9 liters/min. The air flow exit velocities varied from 1.2 to 5.9 m/s at room temperature (25°C). The equivalence ratio was thus varied between 1 and 1.25. Good mixing was ensured by injecting the air and fuel through multiple small holes and passing the mixture through several fine screens. The Reynolds number range was 1500 to 7500, based on the exit diameter, exit air velocity, and the kinematic viscosity of air at room temperature. The initial velocity rms level measured with a hot wire anemometer at the exit of the nozzle on the centerline was 2%.

The flow was excited by an acoustic driver mounted at the end of the pipe opposite the orifice. The speaker was driven

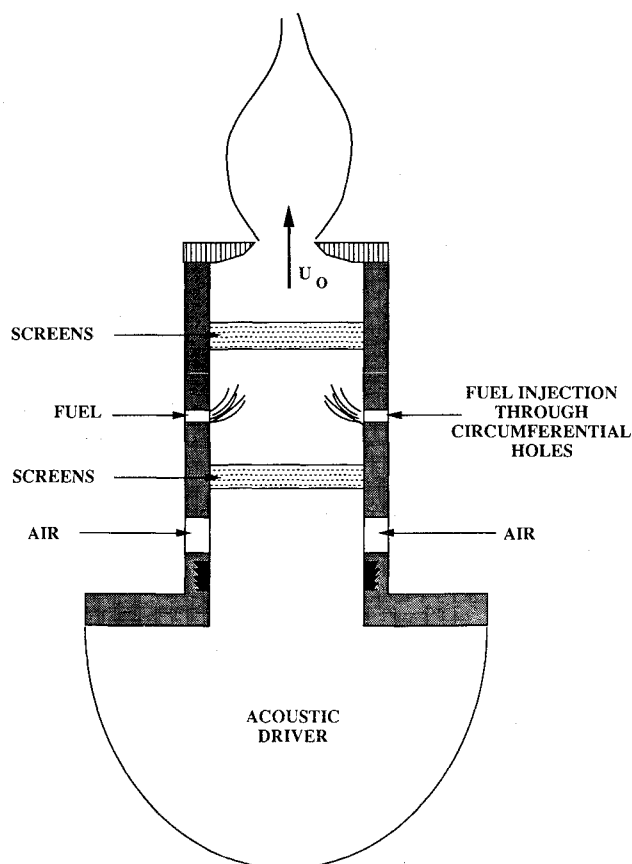


Fig. 1 Experimental setup.

at controlled frequencies and amplitudes using an AM function generator and an audio power amplifier. The forcing frequencies and amplitudes were monitored (in cold flow) by using a calibrated hot-wire anemometer which was also used to measure the mean and turbulent velocities of the air. Previous results showed that the speakers force, and phase lock, only the longitudinal mode of the jet. The maximal forcing level used was 30% rms of the exit mean velocity.

Spectral analysis was performed by a dual-channel frequency domain dynamic analyzer. Its sampling rate is 2.56 times the full-scale frequency range and the resolution was 400 lines on each analysis range. Each channel processes a 1024-point transform. The averaging time changed from test to test and is indicated in the figures.

Natural chemiluminescence emission from CH and C_2 radicals was monitored with an unfiltered photodiode. CH radical ($A^2\Delta-X^2\Pi$) emission was selected with a 430-nm interference filter and monitored with a photodiode. The photodiode bandwidth was greater than 100 kHz. A simple flame height monitor was implemented in the following manner. The flame was imaged onto a 1-cm diameter frosted glass plate directly in front of the photodiode such that when the flame was attached a large area of combustion was seen by the photodiode. As the flame lifted, less and less of the image covered the photodiode, thereby leading to a decreasing signal proportional to flame liftoff height (see inset to Fig. 5). The technique used for height detection yields only averaged value of the liftoff distance, but is advantageous to the control system by reducing the turbulence-induced noise level.

A detailed description of the control system is given in the following section after describing the underlying principles.

Results and Discussion

Open-Loop Control

Open-loop control tests were performed to stabilize the combustion at the lean flammability limit.⁶ The mixture ratio and flow rate were adjusted to obtain a stable lifted flame as shown in Fig. 2a. The instantaneous planar laser-induced fluorescence (PLIF) image of OH shows that the flame is lifted to a height of nearly 1 diameter from the flameholder. The flame is being held by vortices generated in the jet shear layer due to Kelvin-Helmholtz instability.³ It was suggested that the flame can be restabilized at the flameholder if the natural growth of the large-scale structures is disrupted.⁶ The evolution of these vortices is related to the growth of the shear layer, which can be suppressed by forcing it at its initial instability frequency.¹⁶ This forcing generates small-scale vortices commensurate with the initial boundary-layer thickness. By reinforcing these vortices, the shear layer remains nearly at a constant width and the generation of large-scale structures is delayed.

A small forcing level, corresponding to 0.7% of the mean velocity, results in partial stabilization of the flame (Fig. 2b), which is now holding at a smaller liftoff height. Further increase of the forcing to 11% and 19% (Fig. 2, c and d, respectively) results in an improved stability and higher combustion rate, as indicated by the higher concentration of OH at the vicinity of the flameholder. The increased stability results also in an extended flammability limit. For a given fuel flow rate, the air flow rate can be increased considerably, relative to an unforced condition, before blowout of the flame.

The effectiveness of the forcing frequency is highest in the band of the unstable frequencies in the shear layer. Figure 3 shows that the highest increase of air flow velocity before blowout is obtained for a $St_\theta = (f \cdot \theta_0)/U_0 = 0.02$ (where f is the excitation frequency, θ_0 is the initial momentum thickness, and U_0 is the exit velocity of the air), which is within the range predicted by the linear stability theory.^{2,17} This frequency was not dependent on the fuel flow rate. This optimal excitation frequency, identified from the open-loop control, was selected to be used in the closed-loop control system.

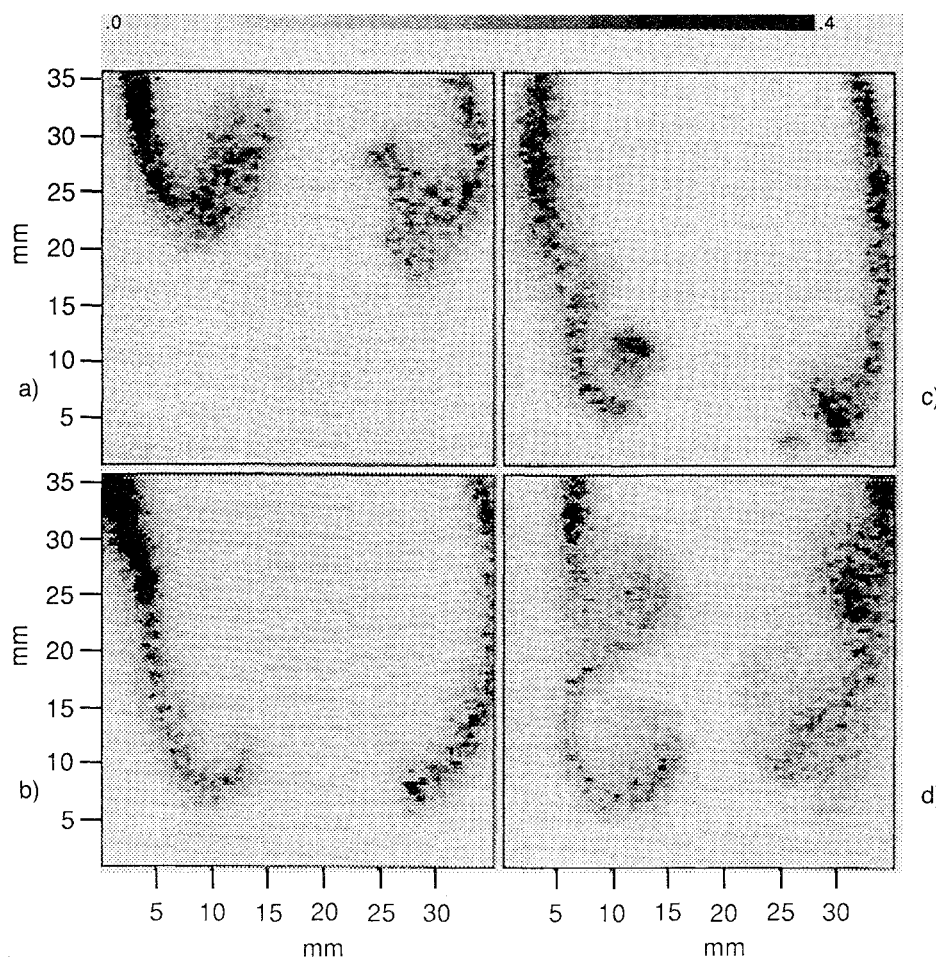


Fig. 2 Instantaneous (18 ns) PLIF OH images of reacting jet forced at $St_\theta = 0.012$, $\phi = 1.34$, $U_0 = 2$ m/s: a) unforced; b) 0.7% forcing; c) 11%; d) 19%. Flameholder is at x axis.

Closed-Loop Control

The objective of the closed-loop control system was to stabilize the flame at any given set-point height relative to the flameholder with sufficiently fast time response to changes in either the set-point or the operating conditions such as change of flow rate or mixture ratio.

The controlled plant consists of three subsystems: acoustics, flow dynamics, and combustion. All the subsystems have links and are interdependent. The output of the plant, i.e., flame standoff, is monitored by sensors and is being fed back and compared with the set-point conditions which subsequently are used as inputs to generate the necessary commands by the controller. A major component of the system is the sensing element that is used as a flame liftoff height detector. The sensor is monitoring the combustion process by imaging the C_2 and CH chemiluminescence emission from the flame. An example of the CH emission range (0.4 ms exposure time) of a forced flame is shown in Fig. 4. The periodic structure of the combustion, indicated by concentrated regions of CH emission, is closely tied to the vortex structures in the flow. The sensing element in the present system, which is a photodiode, integrates the image of the flame over a predetermined active area to determine the flame location (see inset to Fig. 5). The photodiode field of view covers an area from the flameholder to a downstream distance of $1\frac{1}{2}$ diameters, which is the highest flame liftoff height. The CH/ C_2 emission signal is highest when the flame is attached to the flameholder (Fig. 6) and lowest when the flame is lifted off. Thus, the photodiode voltage is proportional to the flame liftoff height. This signal is then compared with the desired height, which is determined by the set-point bias (Fig. 5). The difference between the two signals is used to modulate the amplitude of

the carrier frequency. This frequency is the one determined from the open-loop tests to be the most effective in stabilizing the flame. The modulated frequency drives the speaker in the flame cavity via an audio amplifier. The low-pass filter (LPF) in Fig. 5 is used to check the effect of filtering high-frequency noise on the system stability, and the square wave generator is used to determine the system time response to abrupt changes in the height set point. Both tests are described in detail in the following sections. The spectrum analyzer was used to calculate transfer functions and for spectral analysis. For measuring transfer function, the switch is shifted to open-loop operation. The spectrum analyzer supplies a bandwidth limited white noise which is used to modulate the amplitude of the carrier frequency. The modulated signal is used to drive the speaker. The output of the height detector (channel B) is thus compared with the white-noise input (channel A) to compute the transfer function.

An example of the sensor output signal (corresponding to the flame height) and the speaker's driving signal are shown in Fig. 7, top and bottom, respectively. High sensor signal corresponds to a flame height below the desired set point, which requires a lower control signal amplitude. A lower sensor signal corresponds to a flame lifted above the desired set point which requires a higher control signal amplitude to bring it back down. The apparent oscillations in the two signals are related to the marginal stability of the system as described in the following section.

Transfer Functions (System Stability)

Stability analysis of the system was done using the Bode method. The carrier frequency was modulated with bandwidth limited noise and the corresponding response of the

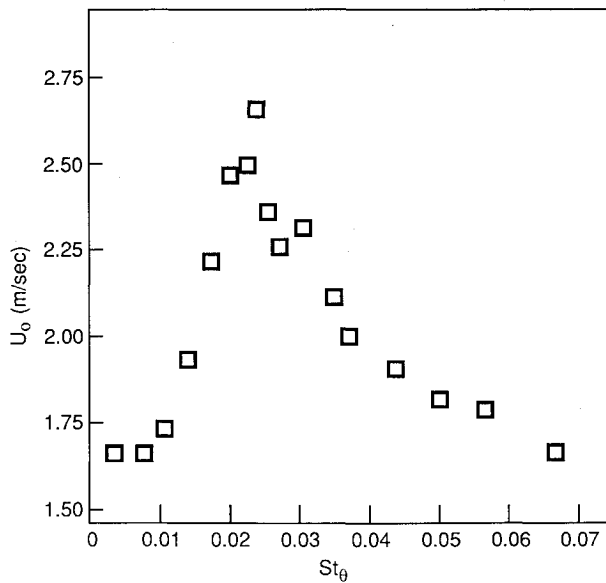


Fig. 3 Optimal increase of lean blowout flammability limit.

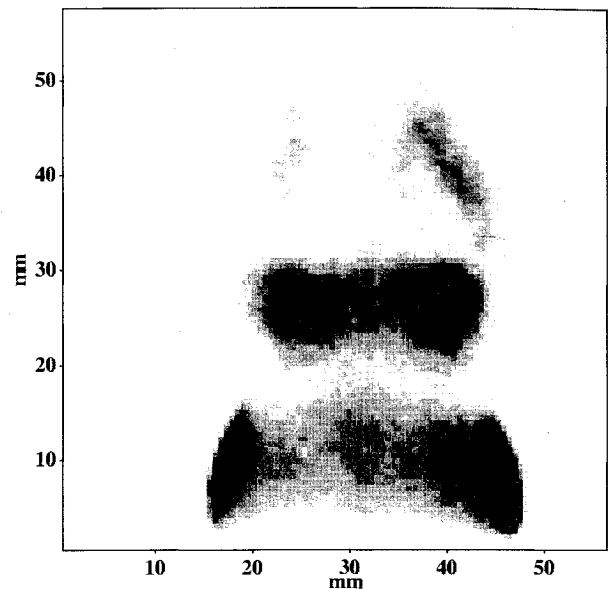
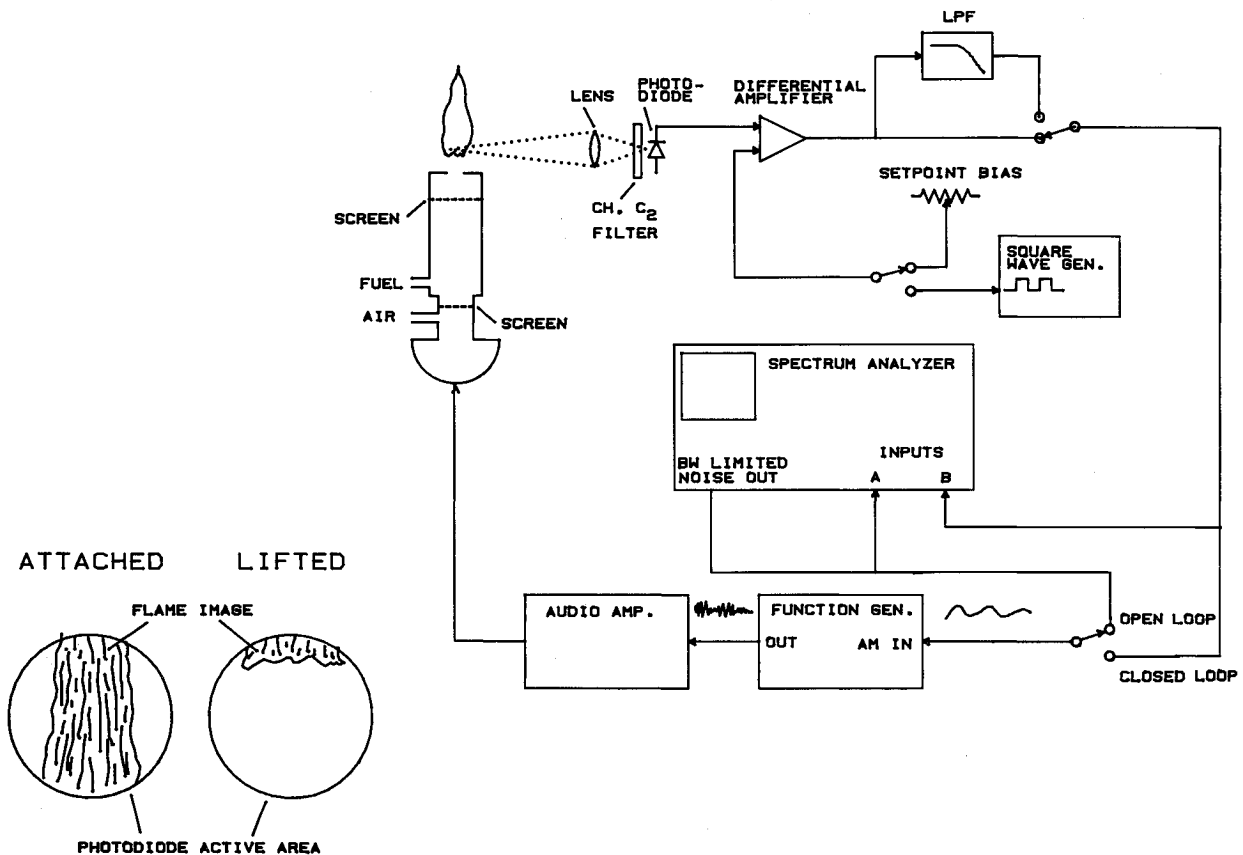
Fig. 4 CH chemiluminescence of the flame forced at $St_0 = 0.02$.

Fig. 5 Detailed schematic of the closed-loop control system with an inset describing the height detector.

sensor was measured. The resulting Bode plot is shown in Fig. 8. The phase of the transfer function, shown in the upper scroll display is defined as

$$\phi = \tan^{-1} \left(\frac{\overline{G}_{BA \text{ IMAG}}}{\overline{G}_{BA \text{ REAL}}} \right) =$$

where \overline{G}_{BA} is the averaged cross-spectrum between the height detector signal and the driving noise signal. The magnitude of the transfer function shown in the lower scroll display is

defined as:

$$|TF| = \sqrt{\left(\frac{\overline{G}_{BA \text{ REAL}}}{\overline{G}_{AA}} \right)^2 + \left(\frac{\overline{G}_{BA \text{ IMAG}}}{\overline{G}_{AA}} \right)^2}$$

where \overline{G}_{AA} is the power spectrum of the driving signal. The data in the plot were averaged over 209 s to extract the relevant information from the highly noisy system. In order to appreciate the amount of noise, a similar plot averaged for 1 s is

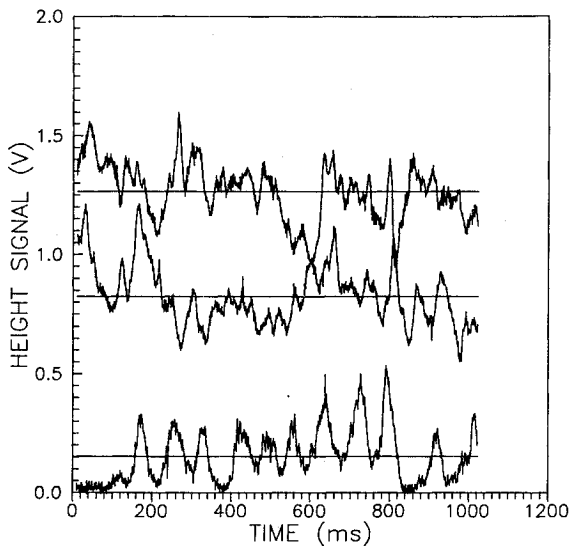


Fig. 6 Time traces of the height detector signal at three liftoff heights of the flame.

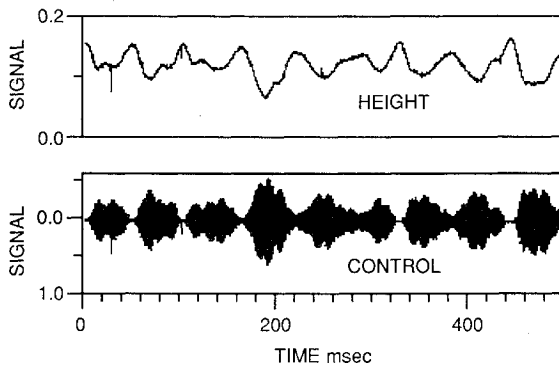


Fig. 7 Time traces of the height detector (top) and the amplitude-modulated speaker's driving signal (bottom) for closed-loop control operation.

shown in Fig. 9. It is obvious that only the long average plot has information that can be analyzed. The high noise level of the system is also demonstrated by the coherence function, depicted also in Fig. 9, which was normally lower than 0.3. The coherence function γ^2 was defined as

$$\gamma^2 = \frac{|\overline{G}_{BA}|^2}{\overline{G}_{AA}\overline{G}_{BB}}$$

where \overline{G}_{AA} and \overline{G}_{BB} are the averaged power spectra of the driving and sensor signals, respectively. The quasilinear drop of the phase angle with frequency indicates a time lag in the system. The 180-deg phase shift occurs over a frequency range of about 18 Hz, which translates to a time lag of 28 ms. Physically, this time lag relates to the convective velocity of the combustible mixture. The acoustic time delay inside the cavity is only of the order of 1 ms. However, when the flame is lifted, the convection time of the vortices from the nozzle to the flame is of the order of 28 ms. To obtain wide stability margins, the gain of the system has to fall below zero decibels before the phase acquires a shift of 180 deg. In the present system, the gain falls relatively slowly, and considering the fluctuations in the gain due to turbulence noise, it still has an intermittent positive gain at the phase crossover point (Fig. 9). This yields a marginally stable system as was depicted in Fig. 7. The spectrum of the CH/C₂ emission signal shows a

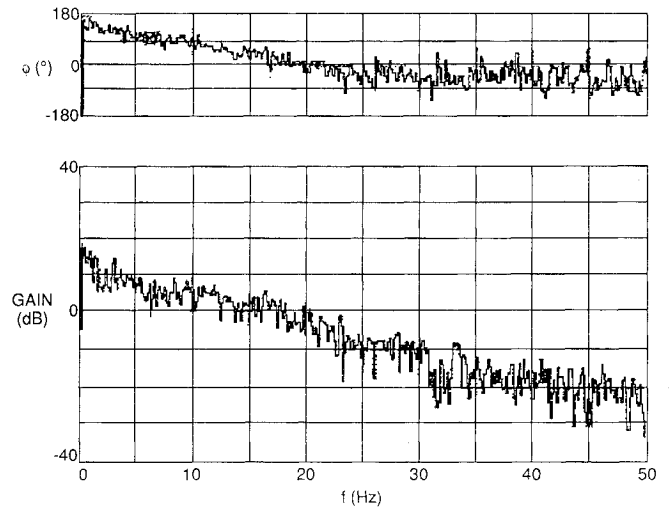


Fig. 8 Averaged Bode plot of the closed-loop system. The upper scroll display shows the phase of the transfer function and the lower depicts the magnitude. $U_0 = 2.23$ m/s, $\phi = 1.25$. Flame at the maximum liftoff distance. Averaging time = 209 s.

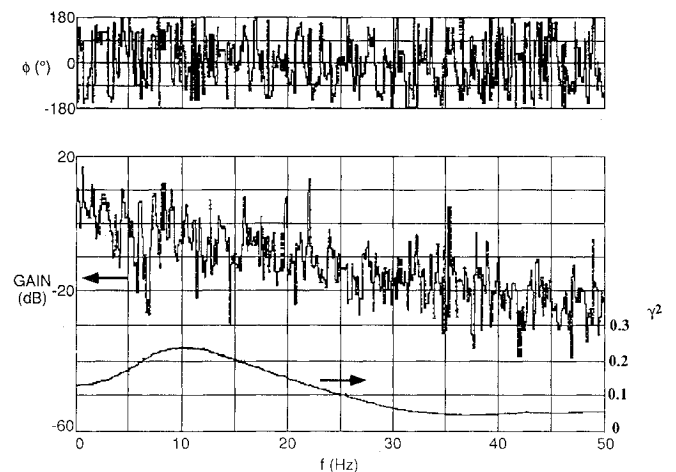


Fig. 9 Short-time-averaged Bode plot of the closed-loop system. Graph description is the same as in Fig. 9. $U_0 = 2.23$ m/s, $\phi = 1.25$. Flame at the maximum liftoff distance. Averaging time = 1 s. Also shown the coherence function (γ^2) between the driving signal and the height detector.

hump at a frequency of 18 Hz, corresponding to the phase crossover point (Fig. 10). This ability to predict the behavior of the system using linear control theory, in spite of its high noise level, is one of the interesting outcomes of the present work.

To demonstrate the influence of the convective time lag, the Bode diagram was replotted for conditions at which the flame was situated closer to the flameholder relative to the previous case (Fig. 8), resulting in a shorter convective time lag. The Bode plot depicted in Fig. 11 shows a slower change in the phase angle, with a 180-deg shift at 40 Hz, corresponding to nearly half the previous convection time. The gain crossing of zero decibels remains at the same frequency. The stability margin for this condition is improved as the gain drops below unity before a phase shift of 180 deg occurs.

The need to reduce the gain at high frequencies, to avoid positive gain at phase shift angles higher than 180 deg, and the general requirement to reduce high-frequency noise, suggest the use of a low-pass filter. Figure 5 shows how this filter was incorporated in the present system. The resulting Bode

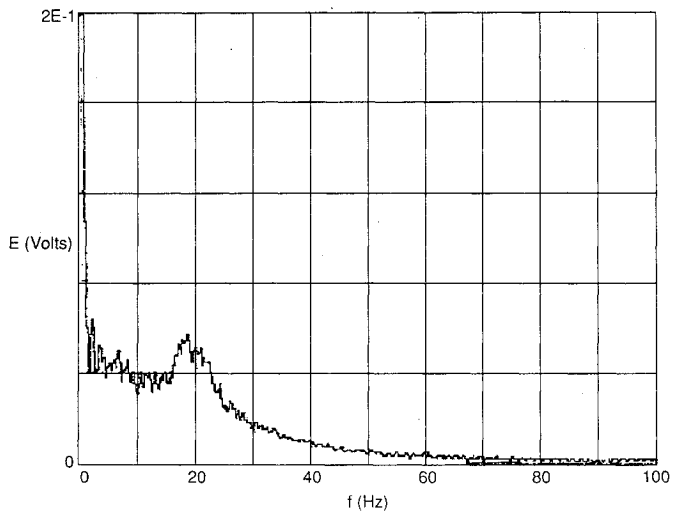


Fig. 10 Spectral distribution of the height fluctuations, indicating flame liftoff instability at 18 Hz. Averaged over 64 s. Conditions same as in Fig. 8.

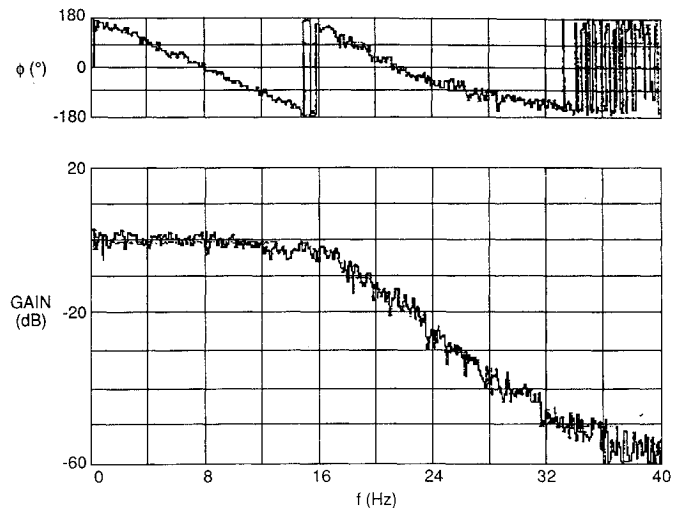


Fig. 12 Bode plot of the closed-loop control system with a low-pass filter (Cutoff frequency 18 Hz). Upper scroll display, transfer function phase; lower display, magnitude. Conditions same as Fig. 8. Averaging time = 286 s.

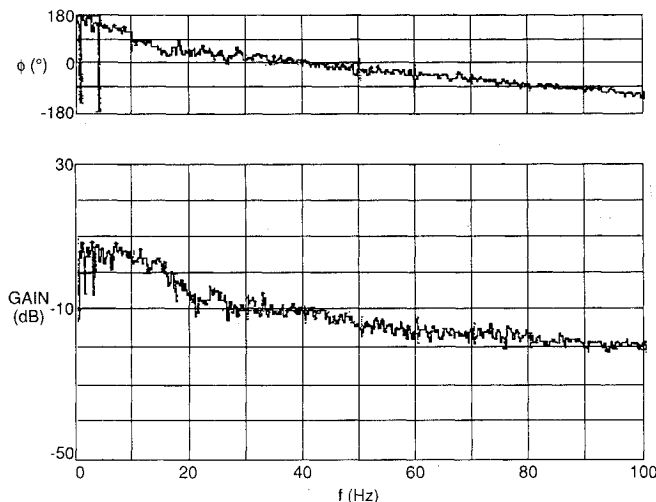


Fig. 11 Averaged Bode plot of the closed-loop system. Upper scroll display, transfer function phase; lower display, magnitude. $U_0 = 2.23$ m/s, $\phi = 1.25$. Flame close to flameholder. Averaging time = 352 s.

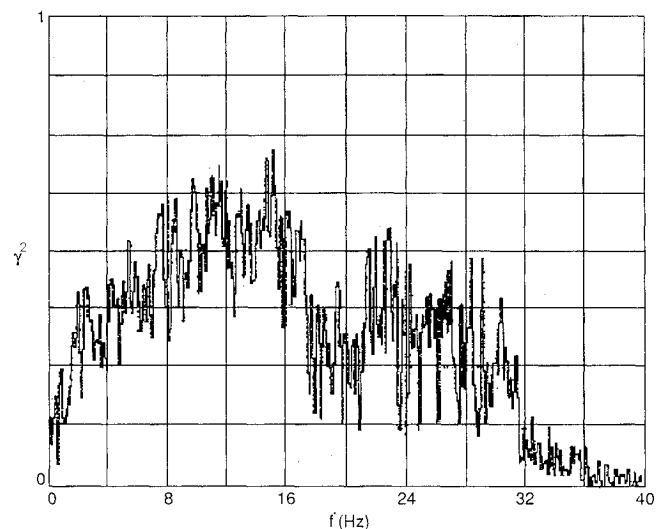


Fig. 13 Coherence function (γ^2) of the driving signal and the height detector. Conditions same as in Fig. 12.

plot is shown in Fig. 12 and the corresponding coherence function in Fig. 13. The improvement in the signal-to-noise ratio is clear from the coherence plot which shows a significant increase up to 0.7. However, the rapid roll-off of the gain at a frequency of 16 Hz is concurrent with an increase in the phase lag, such that 180-deg crossover moves to 8 Hz. Consequently the instability sets off at a lower frequency of 8 Hz as shown in the spectrum of the sensor signal in Fig. 14. For this condition, the flame becomes highly unstable, detaching and reattaching to the flameholder at a nearly steady frequency of 8 Hz. The instability frequency of the closed-loop system can be varied by changing the low-pass cutoff filter frequency, thereby adjusting the amount of added phase lag, and the periodicity of the instability can be predicted accurately from where the phase lag crosses 180 deg.

Response to Changes in Operating Conditions

The response of the closed-loop control system to changes in operating conditions was tested by a step change in the set point (see implementation in the system in Fig. 5) and in the mixture flow rate.

The step change in the height set point was first obtained for an open-loop system (Fig. 15, a and b). The step change in the height set point is manifested in the speaker's driving signal (Fig. 15b) as a sudden change in the modulation amplitude and in the height detector signal (Fig. 15a) as a change in its level. At the time range in Fig. 15, a and b, below 100 ms, the flame sits closer to the flameholder and is released by the open-loop control to go further downstream between 100 ms and 270 ms (approximate numbers for reference only). The time response of the flame to the reduction in the forcing amplitude is about 2 ms, while the response to the increase in amplitude is 15 ms. This difference is another manifestation of the convective time delay; the first change occurs when the flame is located near the flameholder, whereas for the second one the flame is lifted to a larger distance. Another interesting observation is the difference between the rate of change in the two cases. When the flame moves from the low height to the higher, the response rate is only slightly over one-half the rate for the reverse motion. The difference is related to the fact that the motion upstream is caused actively by increasing

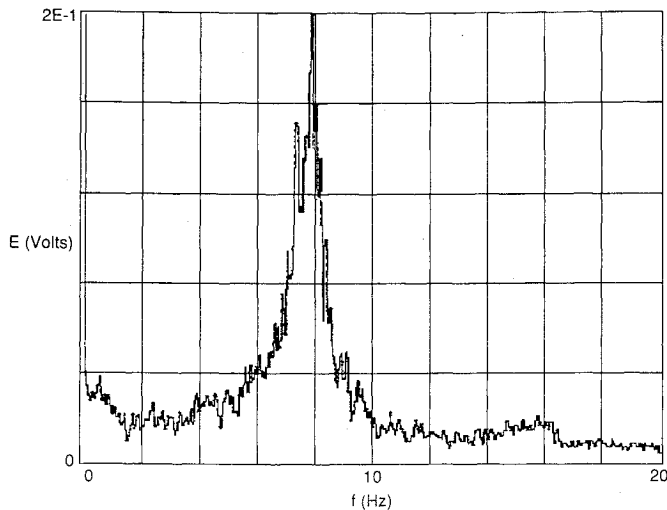


Fig. 14 Spectral distribution of the height fluctuations, indicating flame liftoff instability at 8 Hz. Conditions same as in Fig. 12. Averaged over 91 s.

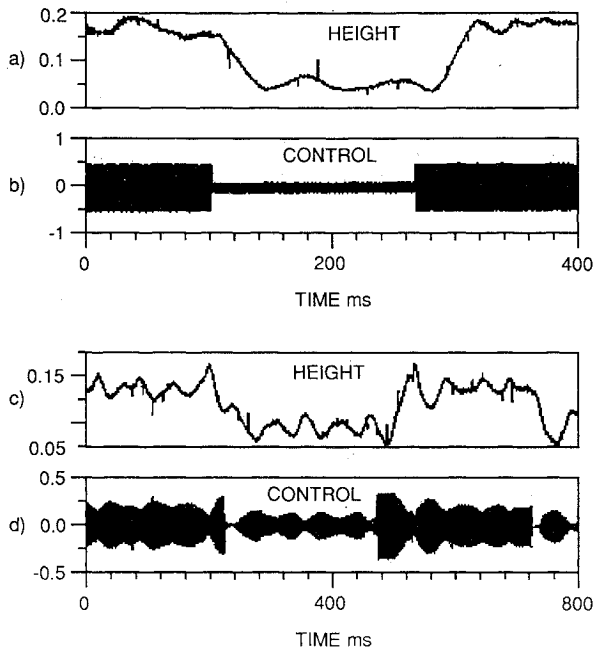


Fig. 15 a) Height detector and b) control signal for a response to step function change in the height set-point open-loop system; c) height detector and d) control signal for a closed-loop system. Conditions same as in Fig. 8.

the forcing level, while for the downstream motion the forcing releases the flame to propagate downstream by itself.

A similar test was conducted with a closed-loop control (Fig. 15, c and d). The control system responds to the rapid changes in the set point by a corresponding change in the modulations. The state of marginal stability of the system is apparent from the oscillations that are superimposed on the sensor (Fig. 15c) and driving signals (Fig. 15d) at a frequency of nearly 18 Hz. The other features of the response are similar to those discussed in relation to the open-loop control.

The system response to sudden changes in the fuel/air mixture flow rate were measured in open (Fig. 16a) and closed-loop operations (Fig. 16, b and c). The air flow exit velocity was increased from 2.3 to 2.9 m/s at $t \approx 800$ ms (both increasing the total flow speed and leaning out the mixture). The open-loop control system (Fig. 16a) could not respond to this change, which destabilized the flame, as evidenced from the sensor

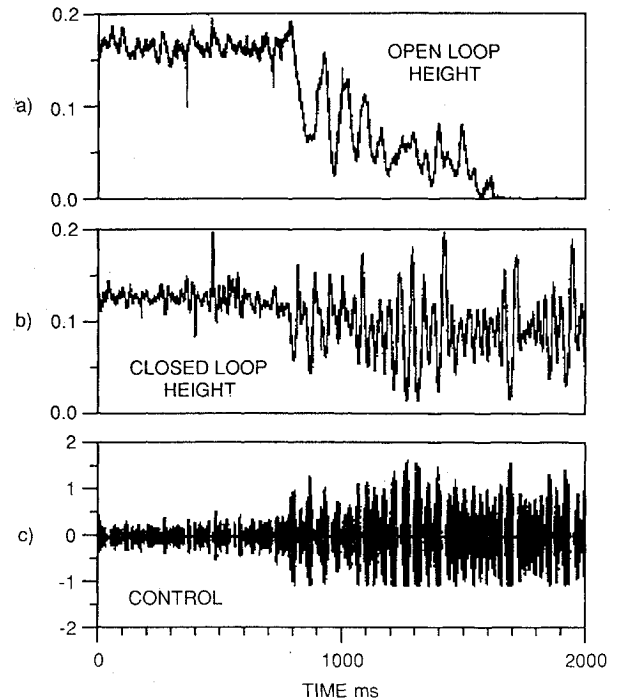


Fig. 16 a) Open-loop response of the height detector to step function change in the air flow exit velocity from 2.3 to 2.9 m/s; b) height detector and c) control signal for the closed-loop response. Equivalence ratio changed from 1.22 to 1. Conditions same as in Fig. 8.

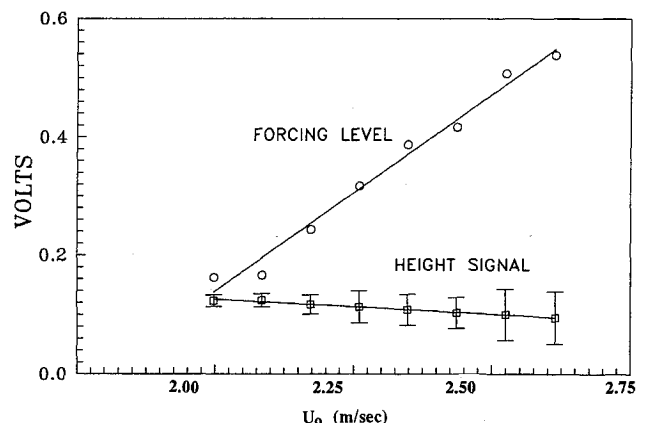


Fig. 17 Change in forcing level of the control and height signals as a function of air flow exit velocity.

signal behavior between 800 to 1600 ms. The instability eventually led to extinction for $t > 1600$ ms. The closed-loop system responded to the same change by increasing the amplitude of the speaker's driving signal (Fig. 16c). The flame was sustained at a flow rate at which it was blown out with an open-loop controller, at the desired height, though with increased fluctuations (Fig. 16b). The closed-loop control system response to changes in air flow rate is summarized in Fig. 17 for a range of air flow exit velocity between 2.06 and 2.76 m/s. The height signal level is nearly constant with a slight drop related to a slight increase in the height, with a concomitant increase in the rms of the fluctuation level around the average height. The forcing level necessary to keep the flame at this constant height increased linearly with the air flow rate.

Summary and Conclusions

The premixed flame exhibits a turbulent nature at the lean flammability limit especially for high fuel flow rates, which lead to high air flow rate and Reynolds number at this condition. Analysis of the dynamic frequency response of the system showed a highly nonlinear system with large noise

level. The nonlinearity of the system is primarily related to nonlinear flow processes in the shear layer such as vortex roll-up and merging. Other control methods that apply phase shift or time delay to the sensor signal require a single frequency linear system. Multiple mode instabilities cannot be handled by a simple phase shift approach; nonlinear systems are controlled by ad hoc methods. In the present tests, the nonlinearity of the system was bypassed by introducing the amplitude modulation control scheme. Open-loop control tests and linear stability theory of shear layers were used to select an effective single frequency for the control signal. By forcing the shear layer at this most amplified frequency, the merging process is suppressed such that the nonlinear mechanism for generating harmonics is eliminated. The forcing is also supplying effectively the required control authority, as demonstrated in open-loop control tests. The response of the lifted flame to this forcing is linear in a certain range, i.e., increased amplitude yields a corresponding linear reduction of the liftoff distance. The linear behavior is restricted at the two extremes: on the lower side by the flameholder and at the downstream side by the blowout limit.

The AM controller did not solve the noise problem; however, surprisingly, the information of long time-averaged Bode or Nyquist plots was sufficient to obtain a good prediction of the system stability margins based on linear control theory.

The stability margins of the system were limited by a convective time lag inherent to the plant due to the finite time which is required for the vortices to be convected from the flameholder to the flame. Attempts to reduce this problem by adding a lead compensation network are hampered by the fact that the improvement in the phase angle is accompanied by an increase in gain at high frequencies which causes reduced stability margins. The time lag problem is alleviated by operating the flame at the utmost upstream location, thus reducing the convective time and reducing the fluctuations level.

Further improvement of the system is planned by applying nonlinear control at the boundaries utilizing a rate feedback controller outside the linear range.

Acknowledgments

The work was supported by ONR, Code 121, J. Hansen. We would like to thank G. Hewer, D. Klabunde, and D. Philbrick for discussions on the control aspects of the work.

References

- ¹Gutmark, E., Parr, T. P., Hanson-Parr, D. M., and Schadow, K. C., "Evolution of Vortical Structures in Flames," *Proceedings of the 22nd International Symposium on Combustion*, Combustion Inst., 1988, pp. 523–529.
- ²Michalke, A., "The Instability of Free Shear Layers," *Progress in Aerospace Sciences*, Vol. 72, Pergamon Press, New York, 1972.
- ³Crow, S., and Champagne, F. M., "Orderly Structure in Jet Turbulence," *Journal of Fluid Mechanics*, Vol. 48, 1971, pp. 547–591.
- ⁴Gutmark, E., Parr, T. P., Hanson-Parr, D. M., and Schadow, K. C., "Planar Imaging of Vortex Dynamics in Flames," *Journal of Heat Transfer*, Vol. III, No. 1, 1989, pp. 148–155.
- ⁵Gutmark, E., Parr, T. P., Hanson-Parr, D. M., and Schadow, K. C., "On the Role of Large and Small Scale Structures in Combustion Control," *Combustion Science and Technology*, Vol. 66, 1989, pp. 107–126.
- ⁶Gutmark, E., Parr, T. P., Hanson-Parr, D. M., and Schadow, K. C., "Stabilization of Combustion by Controlling the Turbulent Shear Flow Structure" *Proceedings of the 7th Symposium on Turbulent Shear Flows*, Stanford Univ., Stanford, CA, Aug. 21–23, 1989.
- ⁷McManus, Vandsburger, V., and Bowman, C. T., "Combustor Performance Enhancement Through Direct Shear Layer Excitation," *Combustion and Flame*, Vol. 82, 1990, pp. 75–92.
- ⁸Flowes Williams, J. E., "Antisound," *Proceedings of the Royal Society of London*, Vol. 395, 1984, pp. 63–88.
- ⁹Flowes Williams, J. E., and Huang, X. Y., "Active Stabilization of Compressor Surge," *Journal of Fluid Mechanics*, Vol. 204, 1989, pp. 245–262.
- ¹⁰Lang, W., Poinso, T., and Candel, S., "Active Control of Combustion Instability," *Combustion and Flame*, Vol. 70, 1987, pp. 281–289.
- ¹¹Poinso, T., Bourienne, F., Candel, S., and Esposito, E., "Suppression of Combustion Instabilities by Active Control," *Journal of Propulsion and Power*, Vol. 5, No. 1, 1989, pp. 14–20.
- ¹²Bloxside, G. J., Dowling, A. P., Hooper, N., and Langhorne, P. J., "Active Control of Reheat Buzz," *AIAA Journal*, Vol. 26, No. 7, 1988, pp. 783–790.
- ¹³Langhorne, P. J., Dowling, A. P., and Hooper, N., "Practical Active Control System for Combustion Oscillations," *Journal of Propulsion and Power*, Vol. 6, No. 3, 1990, pp. 324–333.
- ¹⁴Gulati, A., and Mani, R., "Active Control of Unsteady Combustion-Induced Oscillations," AIAA Paper 90-0270, Jan. 1990.
- ¹⁵Gutmark, E., Parr, T. P., Hanson-Parr, D. M., and Schadow, K. C., "Active Shear Flow Control for Improved Combustion," AIAA Paper 90-0454, Jan. 1990.
- ¹⁶Ho, C. M., and Huerre, P., "Perturbed Free Shear Layers," *Annual Review of Fluid Mechanics*, Vol. 16, 1984, pp. 365–424.
- ¹⁷Gutmark, E., and Ho, C. M., "Preferred Modes and the Spreading Rates of Jets," *Physics of Fluids*, Vol. 26, No. 10, 1983, pp. 2932–2938.